



Published in final edited form as:

Neuroimage. 2009 July 15; 46(4): 998–1003. doi:10.1016/j.neuroimage.2009.03.029.

A MEG investigation of somatosensory processing in the rhesus monkey

Tony W. Wilson^{1,2,3}, Dwayne W. Godwin⁴, Paul W. Czoty⁵, Michael A. Nader⁵, Robert A. Kraft⁶, Nancy C. Buchheimer¹, and James B. Daunais⁵

1Department of Neurology, Wake Forest University School of Medicine

2Department of Neurological Sciences, University of Nebraska Medical Center

3The MEG Center, The Nebraska Medical Center

4Department of Neurobiology & Anatomy, Wake Forest University School of Medicine

5Department of Physiology & Pharmacology, Wake Forest University School of Medicine

6Department of Biomedical Engineering, Wake Forest University School of Medicine

Abstract

The use of minimally and non-invasive neuroimaging methods in animal models has sharply increased over the past decade. Such studies have enhanced understanding of the neural basis of the physical signals quantified by these tools, and have addressed an assortment of fundamental and otherwise intractable questions in neurobiology. To date, these studies have almost exclusively utilized positron-emission tomography or variants of magnetic resonance based imaging. These methods provide largely indirect measures of brain activity and are strongly reliant on intact vasculature and normal blood flow, which is known to be compromised in many clinical conditions. The current study provides the first demonstration of whole-head magnetoencephalography (MEG), a non-invasive and direct measure of neuronal activity, in a rhesus monkey, and in the process supplies the initial data on systems-level dynamics in somatosensory cortices. An adult rhesus monkey underwent three separate studies of tactile stimulation on the pad of the right second or fifth digit as whole-head MEG data were acquired. The neural generators of the primary neuromagnetic components were localized using an equivalent-current-dipole model. Second digit stimulation produced an initial cortical response peaking ~16 ms after stimulus onset in the contralateral somatosensory cortices, with a later response at ~96 ms in an overlapping or nearby neural area with a roughly orthogonal orientation. Stimulation of the fifth digit produced similar results, the main exception being a substantially weaker later response. We believe the 16ms response is likely the monkey homologue of the human M50 response, as both are the earliest cortical response and localize to the contralateral primary somatosensory area. Thus, these data suggest that mechanoreception in nonhuman primates operates substantially faster than that in adult humans. More broadly, these results demonstrate that it is feasible to use current human whole-head MEG instrumentation to record neuromagnetic responses in adult rhesus monkeys. Nonhuman primate models of human disease provide the closest phylogenetic link to humans. The present, non-invasive imaging study could promote exciting links between invasive animal studies and non-invasive human studies, allowing experimentally induced deficits and pharmacological treatments to be interpreted in light of resulting brain network interactions.

Keywords

magnetoencephalography; MEG; monkey; cortex; somatosensory; tactile; drug; alcohol; gamma

Introduction

The emergence of minimally and non-invasive brain imaging techniques, including positron-emission tomography (PET), electroencephalography (EEG), magnetoencephalography (MEG), and functional/structural magnetic resonance imaging (fMRI and sMRI), have revolutionized research in human neuroscience. These imaging tools provide a vehicle for assessing structural parameters such as the gray matter volume of a particular brain region, and/or functional parameters such as the amount of neuronal activity in specific brain areas or the degree of regional interactivity between regions during a behavioral task (Mechelli et al., 2005; Raichle and Mintun, 2006). The utility of these tools for understanding neurological and psychiatric illnesses, brain development, and brain degeneration has been demonstrated repeatedly (Casey et al., 2005; Gur et al., 2007; Strakowski et al., 2005; Thompson et al., 2007). In addition, the application of PET, and to a lesser extent fMRI and MEG/EEG, has been fruitful in expanding knowledge on the time course, mechanism, and regional involvement for a host of pharmacological agents (Malizia, 2006).

Beyond human studies, some of these imaging tools have been used widely in nonhuman primate studies, which has significantly expanded understanding of the tools themselves and a broad array of topics in neurobiology (e.g., Logothetis et al., 2001; Nader and Czoty, 2008; Nader et al., 2008). Studies that have probed more translational questions in neurobiology have primarily employed PET and fMRI. These modalities provide spatially precise estimates of radiotracer-labeled substrate distribution and/or brain activation, although both are derived from blood-flow patterns and thus are indirect measures for which construct validity would be strongly reliant on quasi-normal vasculature and blood-flow (Raichle and Mintun, 2006), which may not always be true. In some cases, the drug or condition of interest (e.g., caffeine or alcoholism) is known to modulate or permanently alter blood-flow through its action on the vasculature which could complicate interpretation from fMRI and PET. MEG- and EEG-based measures, however, are not susceptible to this limitation as both directly measure the electromagnetic activity generated by populations of active neural cells. The limited spatial resolution of non-invasive EEG and the significant variability in intervening tissues across species (e.g., greater scalp muscles in monkey) somewhat restrict its utility in this arena. In contrast, MEG evades these problems through its reliance on the magnetic signature of electrical fluctuations, which is not affected by intervening tissues.

To date, there has been only one published MEG study of nonhuman primates (Teale et al., 1994). That study successfully recorded responses to auditory stimuli from the left hemisphere of an adult pig-tailed macaque using a seven-channel MEG array. Teale and colleagues were able to localize the auditory responses to a portion of the superior temporal gyrus near the monkey auditory cortex, demonstrating that the magnetic fields of electrically active neurons have an adequate signal-to-noise ratio for MEG detection through the relatively dense muscular scalp of the monkey. Although MEG technology has developed tremendously in the past 15 years, to date the Teale et al. (1994) seven-channel MEG study remains the only report of a successful recording in monkey. This is somewhat surprising, particularly since nonhuman primates have been increasingly utilized as translational models of human disease processes (Emborg, 2007; Nader and Czoty, 2005, 2008; Schumacher et al., 1992; Williams et al., 2008).

Considering the benefits conferred by directly quantifying ongoing physiology in time and space, developing MEG for nonhuman primates is of obvious value. Such a capacity would allow the precise study of the neurophysiology underlying a host of diseases ranging from alcohol and substance abuse to cognitive aging, and would constitute an important link between invasive studies in nonhuman primates and non-invasive studies in human subjects. Combining MEG with nonhuman primate models of these diseases would permit longitudinal monitoring of neural activity from the baseline condition (control) through various pharmacological treatments and/or other interventions. In many cases, such manipulations cannot be implemented in human studies due to ethical concerns. Clearly, whole-head studies would be optimally informative with regard to the cortical effects of the construct of interest. Whereas a MEG sensor array designed for monkeys would be the most efficient and efficacious avenue toward this goal, in the absence of a custom-made monkey MEG an attractive alternative is to use the human systems that are now available. In this paper, we demonstrate the use of a human whole-head MEG system to record from an adult rhesus monkey. In doing so, we also report the first MEG data characterizing the spatiotemporal dynamics of monkey somatosensory processing.

Methods and Materials

Animal & Anesthesia Information

MEG recordings were conducted on a six year-old 8.0-kg adult male rhesus monkey (*Macaca mulatta*). The monkey was anesthetized with ketamine (15 mg/kg) and the backs of both legs were shaved for catheter placement. The temple regions on both sides of the head were also shaved for placement of MEG head-localization coils. The monkey was intubated and maintained under 1.5% isoflurane for the duration of the MEG recording session. The animal was covered with a warming gel blanket to maintain body temperature. An angiocatheter (22-gauge) was placed subcutaneously into the saphenous vein for administration of a saline (0.9%) drip. A pulse oximeter was positioned on the animal's toe pad to monitor oxygenation levels and heart rate. ET_{CO2} and isoflurane levels were monitored via a Capnomac (Datex-Ohmeda, Inc.) monitor, which was positioned outside the magnetically-shielded room (MSR). Vital signs were checked every 5 minutes until recovery. The animal was continuously monitored during recordings with a video monitoring system. At the conclusion of the recording procedures the animal was removed from the MSR, recovered from anesthesia, extubated, and returned to its cage.

Experimental Paradigm

Single pneumatic pressure pulses were applied to the volar distal pad of the second (Studies 1-2) or fifth digit (study 3) by means of a 1-cm-diameter rubber bladder encased in plastic housing. Each pressure pulse was of 40-ms duration with a constant inter-stimulus interval of 2.5 s. At least 240 trials per study were collected. After each study, the MSR door was opened so that study team could visually assess the monkey's head position and if necessary re-optimize the head relative to the MEG sensor array.

MEG Data Acquisition

With an acquisition bandwidth of 0.25–150 Hz, neuromagnetic responses were sampled continuously at 600 Hz using a whole-cortex CTF 2005 neuromagnetometer system equipped with 275 first-order axial-gradimeter coils (CTF Systems Inc., Vancouver, BC, Canada). All MEG data were subjected to synthetic third-gradient balancing, which removed or strongly attenuated external non-biological noise sensed by the 29 MEG reference sensors located distant to the cortex. Throughout the recording session, the monkey was strapped to a custom-built Plexiglas plank to aid in positioning and stabilizing the head deep inside the MEG helmet.

Anatomic MRI Acquisition & MEG Coregistration

High resolution structural MRI of the monkey's brain was acquired using a 3T GE MRI scanner. Anesthesia for the MRI scan was identical to that described above for the MEG recording. MRI-visible markers were placed on the three MEG fiducial locations (see below) prior to image acquisition. The animal's head was placed in a specially designed head holder to reduce movement artifact. Fast gradient echo axial, sagittal and coronal localizer images were acquired for graphically prescribing a T1-weighted anatomical scan. Axial high-resolution T1-weighted structural scans with isotropic voxels were acquired with a 3D spoiled gradient echo (3D SPGR) inversion recovery sequence with the following parameters: inversion time (TI) 300 ms, echo time (TE) 2.9 ms, repetition time (TR) 13.6 ms, flip angle 15 degrees, receiver bandwidth 7.8 kHz, in-plane matrix size 256×256 , field of view 12 cm, in-plane resolution 0.47 mm, slice thickness 0.5 mm, number of slices = 128. The 3D SPGR images were acquired six times yielding six sets of images. After acquisition, these images underwent a rigid body alignment and were then averaged.

Prior to MEG, three coils were attached to the head following a conventional three-point fiducial system (nasion and left/right periauricle). Once the monkey was positioned for MEG recording, these coils were energized to induce a magnetic field and thereby allow the coils to be localized in reference to the sensors. The electric current applied to the MEG coils was maintained throughout the recording, which enabled head position to be continuously monitored during each session. Since the coil locations were also known in head coordinates (i.e., referenced to nasion and left/right pre-auricular points), all MEG measurements could be transformed into a common coordinate system based on the spatial relationship of the fiducials with each gradiometer coil location (and orientation). Using this coordinate system, the raw MEG data was coregistered with the monkey's structural MRI volume before source analyses.

MEG Pre-Processing & Source Analyses

The raw MEG signals from each study contained significant cardiac and blood flow artifacts. The latter was likely a product of arterial wall muscle fibers in a vessel analogous to the human vertebral artery. Since the two artifacts had a fixed and virtually coincident temporal relationship, a single orthonormal set of signal-space vectors were extracted using the average sensor-by-sensor topography of the overall artifact. These vectors were scaled to unit vectors prior to forming a matrix for orthogonal projection. Given slight differences in head position between studies, signal-space vectors were defined for each study independently and orthogonal projection was performed on the particular dataset using the study-specific vectors.

MEG data were split into 830-ms epochs, which included a 200-ms pre-stimulus baseline period (-280 to -80 ms). The remaining 80 ms preceding stimulus onset was analyzed identically to that of the post-stimulus period to ensure that early responses were not suppressed. Artifact rejection was based on a fixed threshold method (MEG level > 750 fT), supplemented with visual inspection. For each study, a minimum of 190 trials were time-domain averaged and these signals were filtered (0.3-50 Hz) prior to performing source localization. Source localization was applied using a spherical conductor model that was fit and optimally aligned to the cortical vertex. Contour plots (flux maps) were used to visually identify time periods with clear dipolar field patterns, indicating the presence of an underlying cortical current generated by populations of simultaneously active neurons within a relatively small patch of cortex (Hämäläinen et al., 1993). Each dipolar distribution was modeled as a single equivalent-current-dipole (ECD) using a least-squares fit at the time point of maximum amplitude (i.e., the peak latency). To be accepted, ECDs had to account for at least 80% of the variance in the filtered MEG data. Confidence volumes were estimated for ECDs that reached the GOF criteria using Monte Carlo simulations with 100 iterations, 95% confidence level, and the pre-stimulus baseline period for noise estimation. Each ECD model was also evaluated

using the reduced chi-square metric (Supek and Aine, 1993), but these analyses did not change the results and hence have been omitted for conciseness. The peak field strength measures reported below (i.e., peak amplitudes in fT) correspond to the square root of the sum of squares of the amplitude values for all sensors in the array at the given latency (i.e., vector magnitude). Finally, in addition to the dipole fits described above, a spatiotemporal dipole model was applied to the same responses, but these spatiotemporal fits ultimately failed (i.e., all GOF's < 80%).

Results

Study 1

Stimulation of the right second digit elicited a strong dipolar response that reached a peak amplitude of 194.5 fT 16 ms after stimulus onset (see Figure 1A-B). Source localization indicated a neural generator posterior to the central sulcus of the left hemisphere with an amplitude of 2.04 nAm and a 95% confidence volume of 1.78 cm³ (Figure 1C). A second dipolar response, almost perfectly orthogonal to the first, peaked later at 96 ms in the same part of the MEG array. This neuromagnetic response was considerably weaker, peak amplitude = 94.8 fT, and consequently source localization was not performed. The overall flux pattern, however, suggested a source near the early response but with an orthogonal orientation (Figure 1D).

Study 2

Right second digit stimulation again elicited a dipolar response peaking at 16 ms post-stimulus. The amplitude was 129.6 fT at peak latency (Figure 2). Source localization suggested a generator spatially overlapping with that of Study 1, but the ECD fit explained slightly less than 80% of the variance. A later dipolar response peaking at 96 ms (peak amplitude = 92.5 fT) was again observed. Consistent with Study 1, this response was weaker than the early peak, possessed a similar center of gravity, and had a considerably different source orientation (Figure 2). Due to the low response amplitude, source localization was not attempted.

Study 3

Stimulation of the right fifth digit evoked dipolar fields peaking at 15 ms after stimulus onset with a peak amplitude = 172.1 fT across the MEG array (Figure 3). Dipole localization at 15 ms showed a generator of 1.79 nAm (95% confidence volume: 2.08 cm³) spatially coinciding with the source localized at 16 ms in Study 1. A later and weaker dipolar response was also observed (peak latency = 86 ms, peak amplitude = 78.5 fT). Like that found in Studies 1-2, the field patterns for the late peak were roughly orthogonal to the earlier pattern, but for the fifth digit this later response was slightly earlier and substantially weaker.

Discussion

We evaluated the feasibility of using human, whole-head MEG instrumentation for nonhuman primate investigations, recording the first neuromagnetic responses of rhesus monkey during mechanoreceptive processing. Most importantly, the results establish that existing whole-head MEG instruments can be used for studies in slightly smaller model organisms, such as adult rhesus monkeys. Of course, smaller MEG helmets and sensor radii would improve the spatial resolution of the measurements and more broadly optimize the recording process (e.g., head placement). Beyond feasibility, the results indicated that tactile stimulation of the second digit pad elicits a cortical response peaking ~16 ms after stimulus onset. The results suggest the same stimulation applied to the right fifth digit peaks in the cortex slightly earlier, a finding that will need further study using higher sampling rates. Finally, we localized the neural generators of these tactile responses to an area posterior to the central sulcus. These source

localization results are consistent with somatotopic maps attained invasively in the same species (Pons et al., 1985). Conclusions in regard to the minuscule spatial differences we observed between the fifth and second digit are withheld as this spatial resolution is beyond what is possible using currently available equipment.

The response to tactile stimulation in rhesus monkey has a much more rapid onset than in humans. This was partially expected given earlier work that used electrical stimulation of the median nerve in monkeys (Allison et al., 1989, 1991). These studies suggested the human ~20ms response detected with EEG had roughly a 10 ms peak latency when measured invasively in monkeys, assuming the two responses were in fact cross-species homologues (Allison et al., 1989, 1991). Previous human MEG studies have used tactile stimulation devices, identical to that employed in the current work, in healthy adults (Hoechstetter et al., 2001; Reite et al., 2003) and children (Wilson et al., 2007). The earliest response in humans peaks ~50 ms after stimulus onset and is generated in the somatotopically organized primary somatosensory cortex (S1) of the contralateral hemisphere. The relationship of the human M50 and the monkey M16 is unknown, but the magnetic flux patterns suggest both responses are generated by intraneuronal current flow in the same direction (see field map in (Reite et al., 2003) and present data). In the early 7-channel MEG study of auditory responses, Teale and colleagues (1994) suggested that a M46 response in monkey may correspond to the M100 response in humans (which normally peaks at ~110ms) based on similar criteria and the source location. The M16 reported here is about 3-times faster than the M50 response, which suggests that the relative conduction speeds in the somatosensory and auditory systems differ between the two species. The weaker somatosensory response observed at 96 ms may not have a previously described human homologue. Assuming it was generated in the monkey's left (contralateral) hemisphere, it may be related to the human 85 ms response which is the second and final response in the hemisphere contralateral to stimulation (Hoechstetter et al., 2001).

Our study has particular significance as a bridge between methodologies that allow the use of invasive experimental variables in nonhuman primate models and methodologies that monitor brain activity in human subjects. Studies using non-invasive imaging in animals have typically taken one of two forms. A large body of work has used imaging to understand disease progression or the effects of drug use/abuse. A smaller number of studies have used animal preparations to more clearly identify the biological processes these tools measure. Accordingly, most knowledge concerning the physiological basis of the physical signals quantified by these imaging tools has been derived from work in animals, in which the imaging modality of interest has been combined with invasive electrophysiological recordings. In what is likely the most well-known and thorough example, Logothetis and colleagues (2001) examined the neuronal bases of the blood-oxygen-level-dependent (BOLD) signal that is measured in fMRI studies. They found significant correlations between local-field potential (LFP) measures, multi-unit spiking activity, and the BOLD signal in occipital cortices of anaesthetized rhesus monkeys. Logothetis et al. (2001) reported that LFP measures were the best estimate of spatially coincident BOLD responses, which suggests fMRI activation reflects the intracortical processing and synaptic activity of a neural area rather than its spiking output (Logothetis et al., 2001). Interestingly, a similar visual contrast paradigm was used by Hall and colleagues (2005) in a human MEG study. Consistent with LFP data from the monkey (Logothetis et al., 2001), they reported occipital gamma oscillations increased in amplitude as a linear function of stimulus contrast (Hall et al. 2005). Furthermore, the MEG gamma power response function in human and the analogous LFP function in monkey occipital cortices correlated strongly (Logothetis et al., 2001; Hall et al., 2005). However, more broadly, human MEG studies have benefited relatively less from physiological data derived through animal studies, at least partially due to the absence of simultaneously acquired invasive recordings and MEG in monkeys. Early studies using custom-made micro-SQUID (superconducting quantum interference devices) technology and guinea pig hippocampal slices showed that primary

currents in parallel-oriented pyramidal cells were the dominant source of MEG signals (Okada et al., 1997). Using micro-SQUID technology and an elegant porcine preparation, this group also provided the first empirical evidence that EEG signals, but not MEG signals, are strongly affected by intervening tissues (e.g., skull and scalp; (Okada et al., 1999a; Okada et al., 1999b). More recently, Okada and colleagues have provided single-cell simulation data suggesting action potentials may contribute substantially to MEG signals (Murakami and Okada, 2006), which of course contradicts conventional views of action potentials having a negligible role in the genesis of MEG signals. The capacity to do whole-head recordings in monkeys, as demonstrated here, should expand our understanding of the physiological processes that underlie the MEG signal. For example, whole-head monkey MEG will eventually allow important questions, such as MEG's capacity to resolve temporally coincident sources in nearby but distinct sections of tissue as distinct patches of activity, to be thoroughly addressed using a relatively human-like in vivo model. Likewise, the number of cells and perhaps even the type of cells (e.g., Murakami and Okada, 2006) involved in generating stereotypic human MEG responses could be more fully understood through MEG in monkeys.

Beyond the potential to further understand the biological basis of the methods, perhaps the most important application of non-invasive imaging in animals is that it provides a means to gain a longitudinal understanding of how drugs, diseases, development, and even social situations affect neural structure and function. An example of such a longitudinal analysis is a previous PET imaging study that demonstrated striatal dopamine D2 receptor availability was higher in socially dominant versus subordinate cynomolgus monkeys (Grant et al., 1998; Morgan et al., 2002); these changes in receptor availability had profound influences on behavior as demonstrated by the subsequent findings that cocaine functioned as a reinforcer in subordinate but not dominant monkeys (Morgan et al., 2002). With the addition of MEG, similar studies would provide insight into how dopamine receptor variations modulate local circuit physiology as well as activity in larger-scale neurocognitive systems.

This is the first study to demonstrate the effective use of whole-head MEG in a nonhuman primate. Using MEG, somatosensory responses were mapped to the predicted cortical region, and a marked latency difference was determined in the response to somatosensory stimulation between rhesus monkeys and the reports from human subjects. The implementation of a MEG sensor array designed specially for rhesus monkeys, and the capacity to study behaving monkeys are other longer-term goals. Despite these limitations, the present study demonstrates the feasibility of whole head MEG in nonhuman primates, which should allow for imaging studies that combine the advantages of MEG-derived neurophysiological imaging with the important capability of experimental manipulations that are possible with nonhuman primate models.

Acknowledgments

These studies were supported by NIH grants AA016748 (JBD), DA021658 (PWC), AA16852 and EY18159 (DWG), and DA10584 (MAN). Pilot MEG time was provided by the Department of Diagnostic Neurology, Wake Forest Baptist Medical Center (JBD, TWW).

References

- Allison T, McCarthy G, Wood CC, Jones SJ. Potentials evoked in human and monkey cerebral cortex by stimulation of the median nerve. A review of scalp and intracranial recordings. *Brain* 1991;114:2465–503. [PubMed: 1782527]
- Allison T, McCarthy G, Wood CC, Williamson PD, Spencer DD. Human cortical potentials evoked by stimulation of the median nerve. II Cytoarchitectonic areas generating long-latency activity. *J Neurophysiol* 1989;62:711–22. [PubMed: 2769355]

- Casey BJ, Tottenham N, Liston C, Durston S. Imaging the developing brain: what have we learned about cognitive development? *Trends Cogn Sci* 2005;9:104–10. [PubMed: 15737818]
- Emborg ME. Nonhuman primate models of Parkinson's disease. *ILAR J* 2007;48:339–55. [PubMed: 17712221]
- Grant KA, Shively CA, Nader MA, Ehrenkaufer RL, Line SW, Morton TE, et al. Effect of social status on striatal dopamine D2 receptor binding characteristics in cynomolgus monkeys assessed with positron emission tomography. *Synapse* 1998;29:80–3. [PubMed: 9552177]
- Gur RE, Keshavan MS, Lawrie SM. Deconstructing psychosis with human brain imaging. *Schizophr Bull* 2007;33:921–31. [PubMed: 17548845]
- Hall SD, Holliday IE, Hillebrand A, Singh KD, Furlong PL, Hadjipapas A, Barnes GR. The missing link: Analogous human and primate cortical gamma oscillations. *Neuroimage* 2005;26:13–7. [PubMed: 15862200]
- Hämäläinen M, Hari R, Ilmoniemi RJ, Knuutila J, Lounasmaa OV. Magnetoencephalography-theory, instrumentation, and applications to noninvasive studies of the working human brain. *Reviews of Modern Physics* 1993;65:413.
- Hoehstetter K, Rupp A, Stancak A, Meinck HM, Stippich C, Berg P, et al. Interaction of tactile input in the human primary and secondary somatosensory cortex--a magnetoencephalographic study. *Neuroimage* 2001;14:759–67. [PubMed: 11506548]
- Logothetis NK, Pauls J, Augath M, Trinath T, Oeltermann A. Neurophysiological investigation of the basis of the fMRI signal. *Nature* 2001;412:150–7. [PubMed: 11449264]
- Malizia AL. The role of emission tomography in pharmacokinetic and pharmacodynamic studies in clinical psychopharmacology. *J Psychopharmacol* 2006;20:100–7. [PubMed: 16785278]
- Mechelli A, Price CJ, Friston KJ, Ashburner J. Voxel-Based Morphometry of the Human Brain: Methods and Applications. *Current Medical Imaging Reviews* 2005;1:105–13.
- Morgan D, Grant KA, Gage HD, Mach RH, Kaplan JR, Prioleau O, et al. Social dominance in monkeys: dopamine D2 receptors and cocaine self-administration. *Nat Neurosci* 2002;5:169–74. [PubMed: 11802171]
- Murakami S, Okada Y. Contributions of principal neocortical neurons to magnetoencephalography and electroencephalography signals. *J Physiol* 2006;575(3):925–36. [PubMed: 16613883]
- Nader MA, Czoty PW. PET imaging of dopamine D2 receptors in monkey models of cocaine abuse: genetic predisposition versus environmental modulation. *Am J Psychiatry* 2005;162:1473–82. [PubMed: 16055768]
- Nader MA, Czoty PW. Brain imaging in nonhuman primates: insights into drug addiction. *Ilar J* 2008;49:89–102. [PubMed: 18172336]
- Nader MA, Czoty PW, Gould RW, Riddick NV. Review. Positron emission tomography imaging studies of dopamine receptors in primate models of addiction. *Philos Trans R Soc Lond B Biol Sci* 2008;363:3223–32. [PubMed: 18640923]
- Okada Y, Lahteenmaki A, Xu C. Comparison of MEG and EEG on the basis of somatic evoked responses elicited by stimulation of the snout in the juvenile swine. *Clin Neurophysiol* 1999a;110:214–29. [PubMed: 10210611]
- Okada YC, Lahteenmaki A, Xu C. Experimental analysis of distortion of magnetoencephalography signals by the skull. *Clin Neurophysiol* 1999b;110:230–8. [PubMed: 10210612]
- Okada YC, Wu J, Kyuhou S. Genesis of MEG signals in a mammalian CNS structure. *Electroencephalogr Clin Neurophysiol* 1997;103:474–85. [PubMed: 9368492]
- Pons TP, Garraghty PE, Cusick CG, Kaas JH. The somatotopic organization of area 2 in macaque monkeys. *J Comp Neurol* 1985;241:445–66. [PubMed: 4078042]
- Raichle ME, Mintun MA. Brain work and brain imaging. *Annu Rev Neurosci* 2006;29:449–76. [PubMed: 16776593]
- Reite M, Teale P, Rojas DC, Benkers TL, Carlson J. Anomalous somatosensory cortical localization in schizophrenia. *Am J Psychiatry* 2003;160:2148–53. [PubMed: 14638585]
- Schumacher JM, Hantraye P, Brownell AL, Riche D, Madras BK, Davenport PD, Maziere M, Elmaleh DR, Brownell GL, Isacson O. A primate model of Huntington's disease: functional neural transplantation and CT-guided stereotactic procedures. *Cell Transplant* 1992;1(4):313–22. [PubMed: 1344304]

- Strakowski SM, Delbello MP, Adler CM. The functional neuroanatomy of bipolar disorder: a review of neuroimaging findings. *Mol Psychiatry* 2005;10:105–16. [PubMed: 15340357]
- Supek S, Aine CJ. Simulation studies of multiple dipole neuromagnetic source localization: Model order and limits of source resolution. *IEEE Trans Biomed Eng* 1993;40(6):529–40. [PubMed: 8262534]
- Teale P, Delmore J, Simon J, Reite M. Magnetic auditory source imaging in macaque monkey. *Brain Res Bull* 1994;33:615–20. [PubMed: 8187004]
- Thompson PM, Hayashi KM, Dutton RA, Chiang MC, Leow AD, Sowell ER, et al. Tracking Alzheimer's disease. *Ann N Y Acad Sci* 2007;1097:183–214. [PubMed: 17413023]
- Williams R, Bokhari S, Silverstein P, Pinson D, Kumar A, Buch S. Nonhuman primate models of NeuroAIDS. *J Neurovirol* 2008;14(4):292–300. [PubMed: 18780230]
- Wilson TW, Rojas DC, Teale PD, Hernandez OO, Asherin RM, Reite ML. Aberrant functional organization and maturation in early-onset psychosis: evidence from magnetoencephalography. *Psychiatry Res* 2007;156:59–67. [PubMed: 17728112]

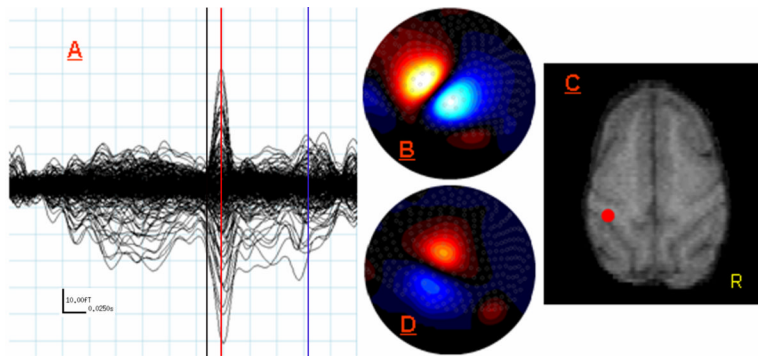


Figure 1.

MEG Data from Study 1: Right Second Digit Tactile Stimulation. (A) Butterfly plot showing all 275 MEG sensors from -180 ms to 145 ms post-stimulus onset. Aqua lines indicate 25 ms (x-axis) by 10 fT (y-axis) increments (see scale in bottom left). The black line indicates stimulus onset (0 ms) and the red line marks the peak latency of the earliest and largest response, which was reached 16 ms after the stimulus onset. The blue vertical line marks the peak latency of the later response at 96 ms. (B) Flux map reflecting field strength gradients across the sensor array at 16 ms. Red represents negative flux and blue represents positive flux. These 2D maps are shown in neurological convention with the front of the MEG helmet oriented toward the top of the figure and the left side of the head on the left. (C) Axial MRI slice on the monkey displayed in neurological convention. The red dot (posterior to the left central sulcus) indicates the spatial location of the ECD computed for the response peaking at 16 ms. (D) Same as (B) except map displays field strength across the array at 96ms (peak latency for later response). Notice the orientation of the current source has rotated almost 90 degrees, but that the center of the zero crossing remains largely the same.

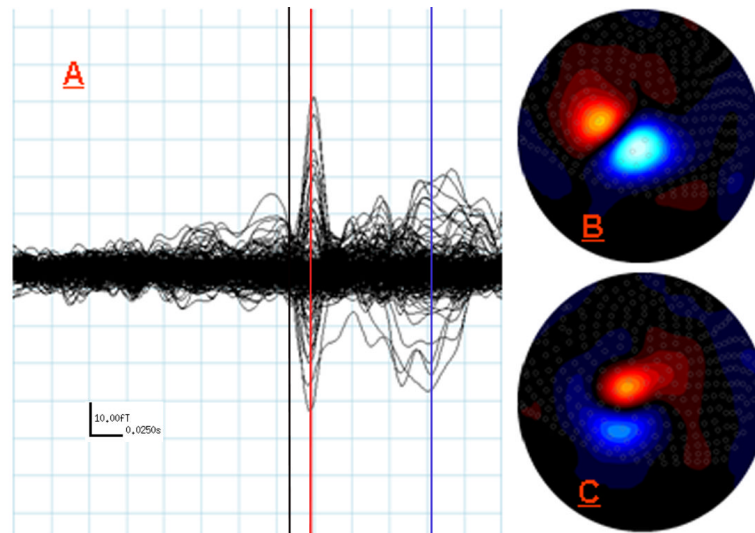


Figure 2. MEG Data from Study 2: Right Second Digit Tactile Stimulation. (A) Butterfly plot of all 275 MEG sensors overlaid from -180 ms to 145 ms post-stimulus onset, with aqua lines representing the same 25 ms (x -axis) and 10 fT (y -axis) increments as in Figure 1 (see scale in bottom left). The black line marks 0 ms (stimulus onset), the red line marks the peak of the earliest and strongest response at 16 ms, and the blue line indicates the peak of the later response at 96 ms. (B) Flux map reflecting field strength gradients across the sensor array at 16 ms. The orientation of the map and the meaning of red and blue are consistent with Figure 1. (C) Same as (B) except map displays field strength across the array at 96 ms (peak latency for later response). Notice the orientation of the current source has again rotated, but that the center of the zero crossing remains the same.

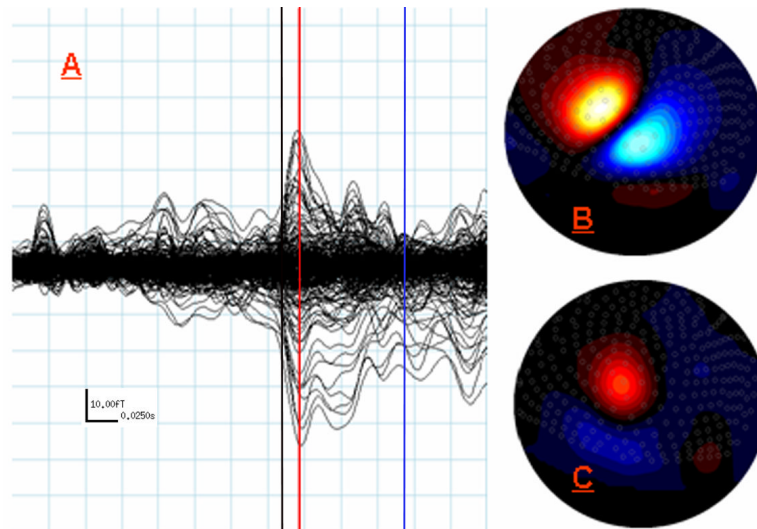


Figure 3. MEG Data from Study 3: Right Fifth Digit Tactile Stimulation. (A) Same as (A) in Figures 1-2, except the red line indicates 15 ms which was the peak of the earliest and strongest response for fifth digit stimulation, and the blue line indicates the peak of the later response at 86 ms (note scale in bottom left). (B) Flux map reflecting field gradients across the sensor array at 15 ms. Orientation and color mapping are consistent with Figures 1-2. (C) Same as (B) except map displays field strength across the array at 86ms (peak latency for later response). Notice overall field strength is considerably weaker than that observed for the later response in Studies 1-2. Although, with respect to the earlier fifth digit response, the center of the zero crossing has rotated roughly orthogonally and the location has remained largely unchanged.